

IDENTIFICATION OF INSULATION DEFECT BY SEQUENTIAL MEASUREMENT OF PARTIAL DISCHARGE IN GIS

Masanobu Yoshida^{1,2*}, Keisuke Suzuki¹, Hiroki Kojima¹
Naoki Hayakawa¹, Masahiro Hanai¹, Hitoshi Okubo¹

¹Nagoya University, Nagoya, Japan

²Chubu Electric Power Co., Nagoya, Japan

*Email: masanobu@okubo.nuee.nagoya-u.ac.jp

Abstract: Though gas insulated switchgear (GIS) has high reliability, the particle invasion into GIS could decrease the insulation reliability. To maintain the insulation reliability, various partial discharge (PD) monitoring techniques have been utilized. In this paper, the authors studied the identification technique for the particle location based on PD measurement, because defect identification is one of the important elements for the risk assessment of GIS. Two kinds of defects (particle in gas or particle on spacer) were set at electrodes in GIS. The phase resolved PD pattern (PRPD pattern) and the temporal transition of the PD pulse number were analyzed. In the case of particle on spacer, temporal change of PD characteristics were observed. On the other hand, steady PD occurrence was observed in the case of particle in gas. We concluded that these changes of PD characteristics were based on the accumulation of the surface charge on epoxy spacer. In other words, we can discriminate the particle condition whether it exists on the spacer or not by analyzing the temporal change of PD characteristics. We proposed the continuous PD monitoring for the reliable PD diagnosis and the identification of insulation defect in GIS.

1 INTRODUCTION

In gas insulated switchgears (GIS), high voltage parts are housed in a sealed tank. When there are defects in GIS, it is not easy to detect them from the outside. Most defects in GIS accompany the occurrence of the partial discharge (PD), PD measurement technique is often applied to detect defects in GIS [1-3]. The identification method of defect type in GIS is also being researched [4-6].

However, even with the same type of defects, measured data differ with the particle size, location, the sensitivity of measurement equipment and so on. In this paper, we studied on improvement of the identification technique for the defect type based on PD activity.

2 EXPERIMENTAL SETUP

2.1 Electrode setup

Two types of defects were examined as shown in Figure 1: a metallic particle on an electrode (particle in gas) and a metallic particle adhered to an epoxy plate (particle on spacer). The relative permittivity of epoxy plate was 6.0. The end of the metallic particle (copper) was cut off with right angle. The defect was set between parallel-plane electrodes (gap length: 60 mm) in SF₆ gas of 0.4 MPa (absolute pressure). PD was generated by applying ac 120 kV_{rms} to the upper plane electrode. The average electric field strength without defects (2 kV_{rms}/mm) was comparable with the operating field strength on the high voltage conductor surface of an actual GIS. The partial discharge inception voltage (PDIV) of each defect was 31–120 kV_{rms} as shown in Table 1. PDIV is measured by gradually voltage increasing until the PD is first detected.

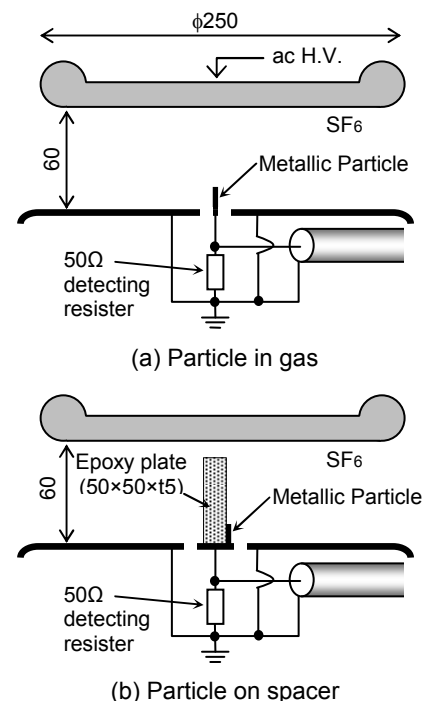


Figure 1: Electrode setup.

Table 1: PDIV for various condition of particle defect

Diameter D (mm)	Length L (mm)	PDIV (kV _{rms})	
		Particle in gas	Particle on spacer
0.25	10	31	-
	5	58	48
	3	75	60
0.45	3	120	100

2.2 Partial discharge measuring circuit

PD current waveforms were measured by using digital oscilloscope (4 GHz, 20 GS/s, 32 MWord) and a personal computer as shown in Figure 2. PD current pulses in SF₆ gas have the rise time of sub-nanoseconds [8,9]. Such PD pulses were detected by this system with the sensitivity of 0.1 pC. As the digital oscilloscope has a large memory capacity, the system can record 6,000 – 10,000 waveforms of PD current pulses continuously. Applied voltage waveform was used as a reference signal to identify the generating phase angle of each PD pulse [10,11].

Besides, light emissions of PDs were also observed using a digital camera mounted image intensifier. The intensity of the light emitted by single PD is rather weak, and accumulated PD light emission for 60 ac cycles were photographed. In addition, in the case of particle on spacer, we measured the charge distribution on the spacer using the non-contacting electrostatic surface voltmeter.

2.3 Applied voltage waveform

The sudden voltage application method was used to prevent the generation of PD in the process of voltage rising and the charge formation on the epoxy plate. This sudden voltage application method can simulate the moment when a particle adhered to the spacer surface under the operational condition. Figure 3 shows an actual ac waveform and detected PD signal when voltage was suddenly applied.

Note that the polarity of the PD discussed in this paper refers to the polarity of the metallic particle tip, it is the opposite polarity to the voltage waveform applied to the high voltage electrode.

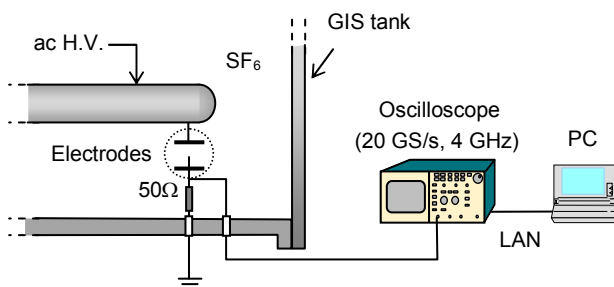


Figure 2: Experimental setup and PD measuring system.

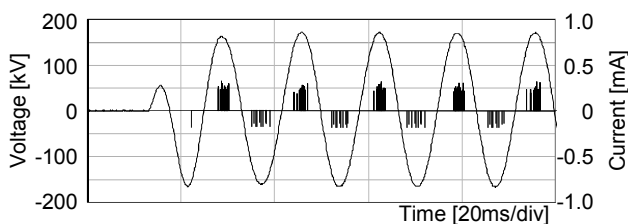


Figure 3: Applied AC voltage wave shape and PD detection.

3 EXPERIMENTAL RESULTS AND DISCUSSION

3.1 Temporal change of PRPD pattern

Figure 4 shows the phase resolved partial discharge pattern (PRPD pattern) in the case of particle in gas at 10 minutes after voltage application ($L = 5\text{mm}$, $D = 0.25\text{mm}$). PD occurred around the peak of applied voltage. This feature of PRPD pattern did not change for the applied time of voltage.

Figure 5 shows the temporal change of the PRPD pattern in the case of particle on spacer ($L = 3\text{mm}$, $D = 0.25\text{mm}$). Figure 5 (a) shows first cycle of PRPD pattern immediately after voltage application. The PRPD pattern was similar to the pattern of the particle in gas case (Figure 4). In Figure 5 (b), at 4 seconds after voltage application, the PD occurrence phase was shifted before the voltage peak and the number of PD pulse was smaller than that in Figure 5 (a). Figure 5 (c) shows the condition at 10 minutes after voltage application, the PD pulse number decreased dramatically, therefore, the feature of PRPD pattern was not obvious.

3.2 Temporal change of PD pulse number

Figure 6 shows the temporal change of the PD pulse number per second (pps). In the case of the particle in gas (Figure 6 (a)), PD occurred constantly. This tendency did not relate to the particle size.

In the case of the particle on spacer (Figure 6 (b)), PDs of several hundreds pps occurred immediately after voltage application. However, pulse number of PD dropped markedly and settled on a constant value (in the case of figure 6 (b), PD pulse number approximate to zero pps.).

Applying voltage for over 2 hours under the same test conditions, no breakdown was observed for both cases.

3.3 Temporal change of charge on insulator

In the case of particle on spacer, temporal change of PD characteristics was thought to be caused by the charge accumulation on the insulator. We measured the temporal change of the surface potential as well as the PD light emission (60 ac cycle's accumulated image) in the case of particle on spacer ($L = 3\text{mm}$, $D = 0.25\text{mm}$).

Figure 7 shows the temporal change of the charge density on the insulator surface, which is measured by the insulator surface potential. The increasing of charge density on the insulator surface around the particle tip was found, as well as an increase in the maximum charge density. In particular the short time constant of the charge accumulation was observed around the needle tip.

We also noticed that the PRPD patterns changed rapidly within a few cycles after voltage application.

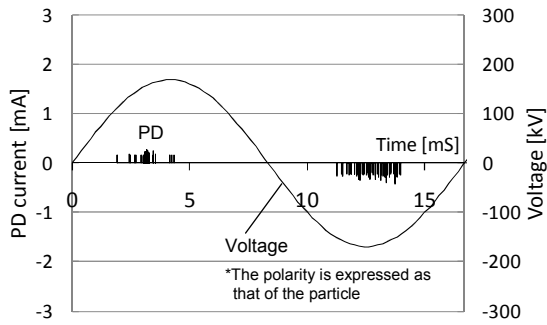
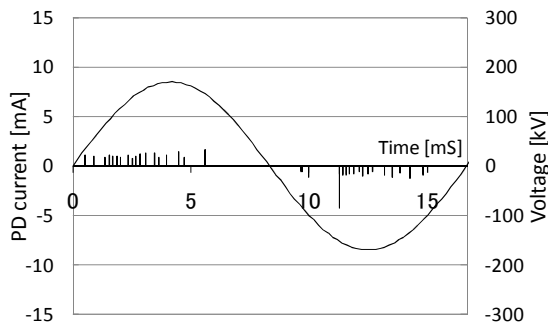
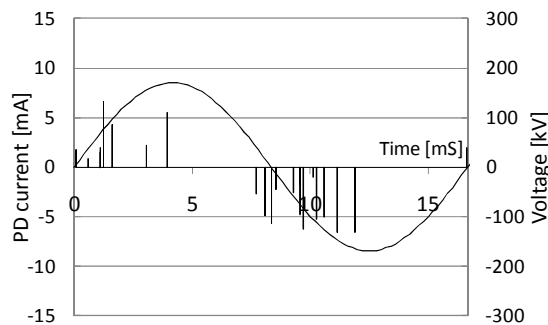


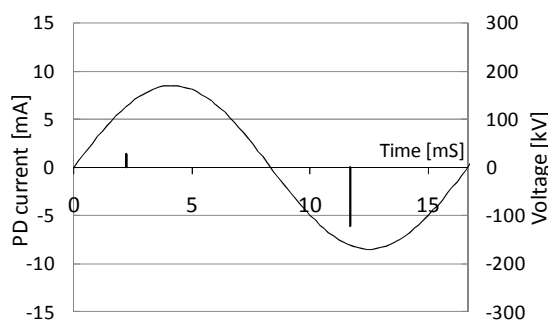
Figure 4: PRPD pattern at 10 minute after voltage application (Particle in gas, $L = 5 \text{ mm}$, $D = 0.25 \text{ mm}$)



(a) Immediately after voltage application



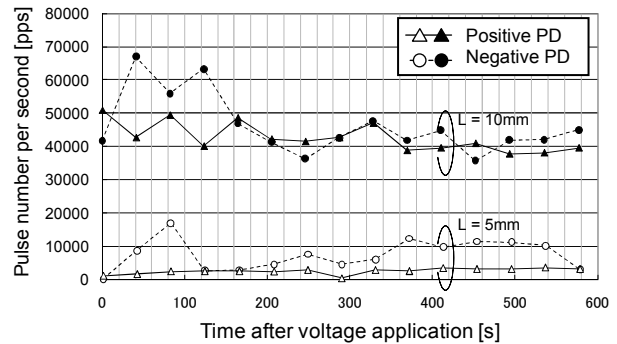
(b) 4 seconds after voltage application



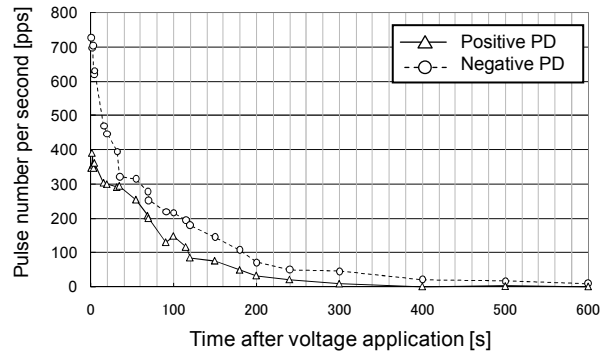
(c) 10 minutes after voltage application

Figure 5: Temporal change of PRPD pattern for a particle on spacer. ($L = 3 \text{ mm}$, $D = 0.25 \text{ mm}$)

It was thought, therefore, that PRPD patterns were strongly influenced by the charge in the immediate area around the metallic particle tip. Figure 8 shows the temporal change of the PD light emission image, PD was occurring around the whole circumference of the particle tip up to 4



(a) Particle in gas ($D = 0.25 \text{ mm}$)



(b) Particle on spacer ($L = 3 \text{ mm}$, $D = 0.25 \text{ mm}$)

Figure 6: Temporal change of PD pulse number after voltage application.

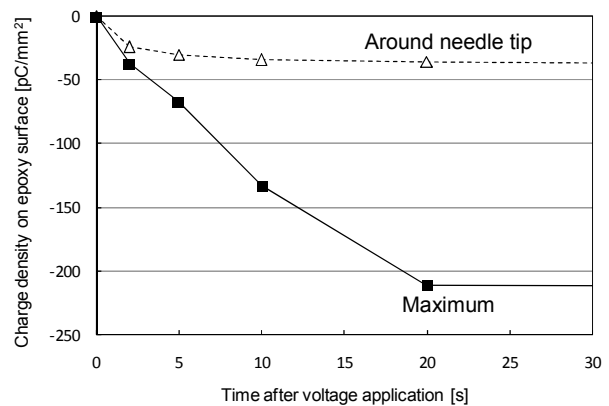


Figure 7: Temporal change of charge density on epoxy surface. ($L = 3 \text{ mm}$, $D = 0.25 \text{ mm}$)

seconds after voltage application. From around 20 seconds after voltage application, however, the PD light intensity in the insulator side gradually became weaker. At 10 minutes after voltage application, it was hard to observe the PD at the insulator side of particle tip. This phenomenon was thought to reveal the reduction of electric field around the needle tip by the formation of the negative charge at the insulator surface.

By contrast, the case of particle in gas, PD occurrence appeared at random locations around the needle tip and any temporal change was not observed.

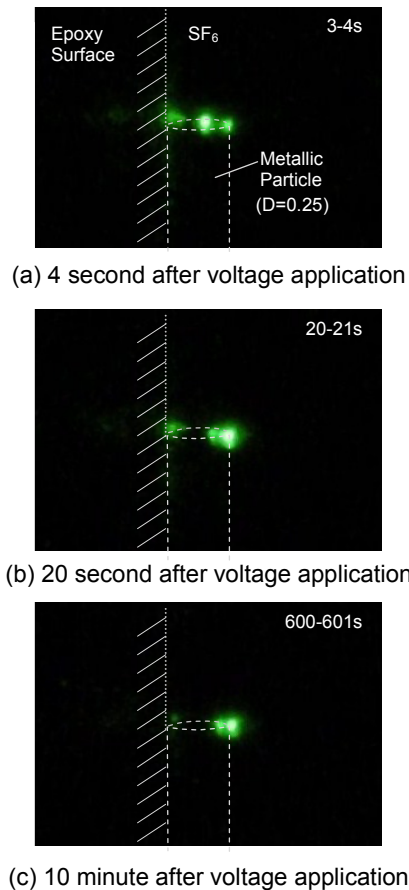


Figure 8: Temporal change of PD light emission image around a particle tip. (Particle on spacer, $L = 3$ mm, $D = 0.25$ mm)

3.4 Influence of charge on spacer for PD activity

In order to investigate the influence of charge on insulator surface for the PD occurrence, the temporal change of the electric field strength around the particle tip was calculated. In this calculation, it was assumed that charges were accumulated in the region of $200\ \mu\text{m}$ in depth in the epoxy plate, and the charge density were equal terms to figure 7.

Figure 9 shows the temporal change of the calculated electric field strength at a position $10\ \mu\text{m}$ away from the metallic particle tip (insulator surface side) under the positive and negative peak of voltage.

In this figure, the electric field around the metal tip reduces over time under negative polarity voltage. This tendency continues up to 20 seconds after voltage application. No less than Figure 7, this reduction of electric field strength would be caused by the negative charge on insulator surface.

Besides, in spite of the electric field increase over time under positive polarity voltage, the PD pulse

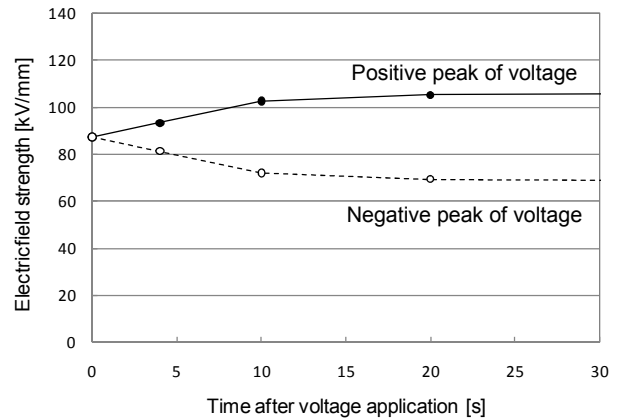


Figure 9: Temporal change of electric field strength at a insulator surface of $10\ \mu\text{m}$ away from needle tip. ($L = 3$ mm, $D = 0.25$ mm)

number decreased as shown in Figure 6 (b). The reason of this paradox was not made clear, there is a possibility that related to the decrease of negative PD over time.

From the findings above, we consider that the temporal change of PRPD pattern and PD pulse number reveal the change of PD mechanism caused by charge accumulation on insulator. In other words, in order to identify the defect type based on PD measurement, temporal analysis of the PD characteristics is one of the effective means.

3.5 Time constant analysis of PD activity in the case of particle on spacer

Temporal change of PD was observed within dozens of second, and it shows the importance of continuous PD monitoring for the reliable PD diagnosis and the identification of insulation defect in GIS.

Figure 10 shows the temporal change of PD for different particle sizes. The vertical axis of figure 10 shows the integration of positive or negative charge during 1 second. Table 2 shows the time constant of PD transition with different particle sizes. To calculate the time constant, the fitted curve of exponential function was applied. The small time constant was observed with a particle size of long length and small diameter. In this condition, continuous PD was also observed, it is possible to detect PD. Besides, at a particle size of short length and large diameter, the large time constant was observed. Then, temporal change of PD can be measured by PD measurement with several minutes interval. The particle with $L = 3$ mm, $D = 0.25$ mm was the most severe condition for PD measurement among three cases. Short time interval of PD measurement with dozens of seconds was required for the reliable PD diagnosis and the identification of insulation defect in GIS.

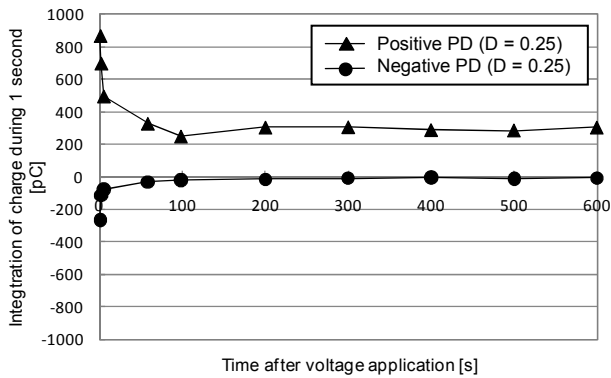
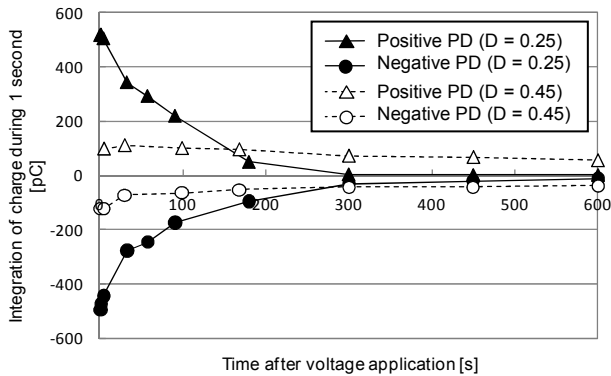

 (a) Particle length $L = 5$ mm

 (b) Particle length $L = 3$ mm

Figure 10: Temporal change of PD for different particle sizes in the case of particle on spacer.

Table 2: Time constant of PD transition for different defect sizes in the case of particle on spacer.

Diameter D (mm)	Length L (mm)	Time constant (s)	
		Positive PD	Negative PD
0.25	5	34	31
	3	77	100
0.45	3	1000	91

4 CONCLUSION

We attempted to establish a method for accurately discrimination whether the particle defect is insulator-mediated or not in SF₆ gas.

We demonstrated that assessing the temporal changes of the PD activity (e.g. PRPD pattern and PD pulse number) is an effective means of accurately identifying the defect type in GIS, because the temporal change of PD characteristics reveals the change of PD mechanism caused by charge accumulation on insulator. The continuous PD monitoring is required for the reliable PD diagnosis and the identification of insulation defect in GIS.

From the time constant analysis, time interval of PD monitoring with dozens of seconds was required for the reliable PD diagnosis and the identification of insulation defect in GIS.

5 REFERENCES

- [1] N.D. Kock, B. Coric, R. Pietsch: "UHF PD detection in gas-insulated switchgear – Suitability and sensitivity of the UHF method in comparison with the IEC 270 method", IEEE EI Magazine, Vol. 12, No. 6, pp. 20 – 25, 1996
- [2] T. Kato, F. Endo, S. Hironaka: "Sensitive partial discharge monitoring system by UHF method and calibration technique", CIGRE GIS symposium, pp.73 - 76, 2001
- [3] CIGRE TF15/33.03.05: "Partial discharge detection system for GIS: Sensitivity verification for the UHF method and the acoustic method", ELECTRA, No. 183, pp. 75 – 87, 1999
- [4] M. Hanai, F. Endo, S. Okabe, T. Kato, H. Hama, M. Nagao: "New development for detecting partial discharge using an UHF method and its application to power apparatus in Japan", CIGRE, D1-106, 2006
- [5] S. Okabe, T. Yamagiwa, H. Okubo, "Detection of harmful metallic particles inside gas insulated switchgear using UHF sensor", IEEE Trans. on DEI, Vol. 15, No. 3, pp. 701 – 709, 2008
- [6] H. Hama, S. Okabe, M. Hanai, T. Rokunohe, H. Okubo, M. Nagao: "Advanced on-site monitoring and diagnostics techniques for gas insulated switchgears", CIGRE, D1-203, 2008
- [7] R.G.A. Zoetmulder, S.Meijer, J.J.Smit, W.van Kampen: "Condition based maintenance of HV switchgear systems", 14th ISH, G-126, 2005
- [8] A.J. Reid, M.D. Judd, B.G. Stewart, R.A. Fouracre: "Partial discharge current pulses in SF₆ and the effect of superposition of their radiometric measurement", J. Phys. D: Appl. Phys., Vol. 39, pp. 4167 – 4177, 2006.
- [9] H. Okubo, N. Hayakawa, A. Matsushita: "The relationship between partial discharge current pulse waveforms and physical mechanisms", IEEE Electr. Insul. Mag., Vol. 18, pp. 38 – 45, 2002.
- [10] H. Okubo, N. Hayakawa, "A novel technique for partial discharge and breakdown investigation based on current pulse waveform analysis", IEEE Trans. on DEI, Vol. 12, No. 4, pp. 736 – 744, 2005
- [11] K. Nishizawa, T. Okusu, H. Kojima, N. Hayakawa, F. Endo, M. Yoshida, K. Uchida, H. Okubo: "Particle size identification in GIS by ultra high speed measurement on partial discharge", CMD, D2-13, 2008